Z. Phys. C 57, 37-42 (1993)

Zeitschrift für Physik C Particles and Fields

Production of slow singly charged fragments in 200 GeV/c hadron nucleus interactions

R. Albrecht[1], T.C. Awes[2], C. Baktash[2], P. Beckmann[3], F. Berger[3], M.A. Bloomer[4], D. Bock[3], R. Bock[1], G. Claesson[5], G. Clewing[3], L. Dragon[3], A. Eklund[5], R. Ferguson[2], A. Franz[6], S.I.A. Garpman[5], R. Glasow[3], H.-Å. Gustafsson[5], H.H. Gutbrod[1], G. Hölker[3], J. Idh[5], P. Jacobs[4], K.-H. Kampert[3], B.W. Kolb[1], H. Löhner[7], I. Lund[7], F.E. Obenshain[2,6], A. Oskarsson[5], I. Otterlund[5], T. Peitzmann[3], F. Plasil[2], A.M. Poskanzer[4], M.L. Purschke[1], H.-G. Ritter[4], B. Roters[1], S. Saini[2], R. Santo[3], H.R. Schmidt[1], S.P. Sorensen[2,6], P. Steinhaeuser[1], K. Steffens[3], E. Stenlund[5], D. Stüken[3], G.R. Young[2]

[1] Gesellschaft für Schwerionenforschung (GSI), Planckstrasse 1, Postfach 110541, W-6100 Darmstadt, Federal Republic of Germany
[2] Oak Ridge National Laboratory (ORNL), POB 2008, Oak Ridge, TN 37831-6372, USA
[3] Institut für Kernphysik, University of Münster, Wilhelm-Klemm-Strasse 9, W-4400 Münster, Federal Republic of Germany
[4] Nuclear Science Division, Lawrence Berkeley Laboratory, Berkeley, CA 94720, USA
[5] Division of Cosmic and Subatomic Physics, Department of Physics, University of Lund, Sölvegatan 14, S-22362 Lund, Sweden
[6] University of Tennessee, Knoxville, TN 37996-1200, USA
[7] KVI, University of Groningen, NL-9747 AA Groningen, The Netherlands

Received 16 July 1992

Abstract. Measurements of slow, singly charged fragments in the target rapidity region have been performed for proton and pion induced reactions with various nuclei at 200 GeV/c. Multiplicity, angular and energy distributions are examined and used to study the effects of rescattering in the nuclear medium. Data are compared to a "geometric cascade model" and to simulations with the VENUS 3.11 and the FRITIOF 1.7 Monte Carlo codes.

1 Introduction

The great interest shown in multiparticle production mechanisms in nucleus-nucleus collisions at ultra-relativistic energies has revived the importance of hadron-hadron and hadron-nucleus interactions [1]. The gross features of the data obtained in the nucleus-nucleus collisions at these high energies can be understood in terms of the collision geometry [2]. One way to get further knowledge of the underlying mechanisms is to study hadron-hadron and hadron-nucleus interactions. This is needed when making more detailed extrapolations to nucleus-nucleus reactions. The characteristic features of hadron-nucleus collisions should in principle be a helpful tool when extracting effects induced by the surrounding nuclear medium. The number of collisions (ν) in hadron-nucleus interactions, sometimes referred to as the nuclear thickness, is believed to be closely correlated to the average number of emitted slow particles, i.e. singly charged nuclear fragments, N_f [3, 4]. Once the hadron has undergone the first collision it is no longer acting as a free hadron but appears as an excited state of hadronic matter whose characteristics are not very well known. It is generally believed that most of the hadronization takes place outside the nuclear medium and that cascading in the nuclear medium is rather limited [5]. The emitted hadrons in these collisions can be divided up into two classes; produced particles (mainly pions) and the slow, target associated fragments. In this work the results from a study of singly charged slow fragments are used to address the questions of their target mass dependence as well as the existence of a cascade in the nuclear medium. Earlier data [6-9] on these subjects obtained with visual track detectors like emulsion or bubble chambers mainly suffered from low statistics. The data presented here is the first high statistics, high granularity measurement of target fragments performed at high energy. There have however been studied at slightly lower energies [10] and in nucleus-nucleus collisions [11].

2 Experimental setup and data analysis

The data on proton and pion induced reactions at 200 GeV/c reported here were taken with the WA80 experimental setup [12] at the CERN SPS. A secondary mixed beam of protons and pions was used, and the signals from gas Cherenkov counters were used to define valid beam triggers for protons and pions. The contamination of other beam particles amongst the accepted triggers are less than one percent. The data were taken with a minimum bias trigger requiring: i) a valid beam particle and ii) at least one accepted charged particle in the pseudorapidity region $1.3 < \eta < 4.2$ measured with the streamer tube multiplicity detectors [13]. For the study of energy- and angular distributions we wanted an essentially background free event sample. To achieve such a sample of events, uncontaminated by background events, we have selected events with high ($E_T > 5$ GeV) trans-

Table 1. General event information for the data presented in this article. The minimum bias sample was used for the multiplicity studies and the high E_T sample were used for studies of angular and energy dependencies

Target	Target thickness (mg/cm^2)	Event sample min bias	Event sample $E_T > 5$ GeV	$\frac{\sigma\,(\text{high } E_T)}{\sigma\,(\text{min bis})}$
p-Au	250	167 408	93 955	17.5 %
p-Ag	200	84 521	40 685	15.3 %
p-Cu	200	168 538	73 493	13.3 %
p-Al	200	127 437	47 103	10.0 %
p-C	209	361 470	162 725	3.0 %
p-No	-	11 735	44	0.13%
π-Au	250	40 567	17 548	10.0 %
π-Ag	200	21 793	7 480	8.6 %
π-Cu	200	37 847	11 571	7.4 %
π-Al	200	29 859	7 836	5.7 %
π-C	209	85 741	34 181	2.0 %
π-No	-	5 626	11	0.03%

verse energy, measured by the mid rapidity calorimeter [14], which has full azimuthal coverage for pseudo-rapidities in the range $2.4 < \eta < 5.5$. For the multiplicity studies, we have chosen to use our minimum bias data with suitable corrections from 'target out' runs. The corrections remove approximately 30% from the events samples. More general information on the data sets is given in Table 1. The results discussed in this work were obtained using the Plastic Ball spectrometer [15] covering the target rapidity region ($-1.7 < \eta < 1.3$). Each of the 655 detector modules is a particle identifying telescope with a ΔE (CaF_2) and E (plastic) detector, which are read out via one common photomultiplier (Phoswich technique). These telescopes have the capability of fully identifying $Z = 1$, 2 fragments from 30–250 A MeV and with the extension up to 400 MeV for protons. This gives us a sample of singly charged fragments that is essentially free from pions and $Z > 1$ fragments. Above this energy the contamination of pions will be too severe to give an acceptable separation between these and the protons. Within the acceptance region the efficiency of 'slow proton' detection is close to 100%, except for angles close to 90 degrees where we suffer from absorption in the target chamber. The occupancy in the most forward of the Plastic Ball modules were 14% in the case of p-Au collisions.

3 Results

Distribution of the multiplicity, N_f, of slow singly charged fragments, hereafter referred to as slow protons, (30 A MeV $< E <$ 400 A MeV), emitted in the target rapidity region ($-1.7 < \eta < 1.3$) for proton and pion induced interactions at 200 GeV/c can be seen in Fig. 1 and 2. The distributions are corrected for 'no target' contribution. To study the shape of the distributions in more detail a simple "geometric cascade model" [3], (GCM), was adopted. The basic idea behind this model is that a single struck target nucleon ($\nu = 1$) produces slow protons according to a geometric distribution:

$$P_1(N_f) = (1 - X)\, X^{N_f} \qquad (1)$$

where

$$X = \frac{\langle N_f \rangle_{\nu=1}}{1 + \langle N_f \rangle_{\nu=1}}. \qquad (2)$$

This assumes that collisions between the projectile hadron and any target nucleon yields, on the average, the same number of slow protons. The validity of such an assumption was confirmed in a neutrino-nucleus bubble chamber experiment [16] at Fermilab and this model was also able to describe the data of De Marzo et al. [8] ($p - A$ interactions at 200 GeV/c), Rees et al. [9] ($\pi^{\pm}$-Ne at 30 and 64 GeV/c) and Faessler, Braune et al. [10] (hadron-A at 20, 37, 50, 100 and 150 GeV/c).

In order to consider all collisions that the incoming hadron undergoes in the target nucleus we have to estimate the distribution of the number of collisions (ν). This was calculated using a frozen straight line geometry and

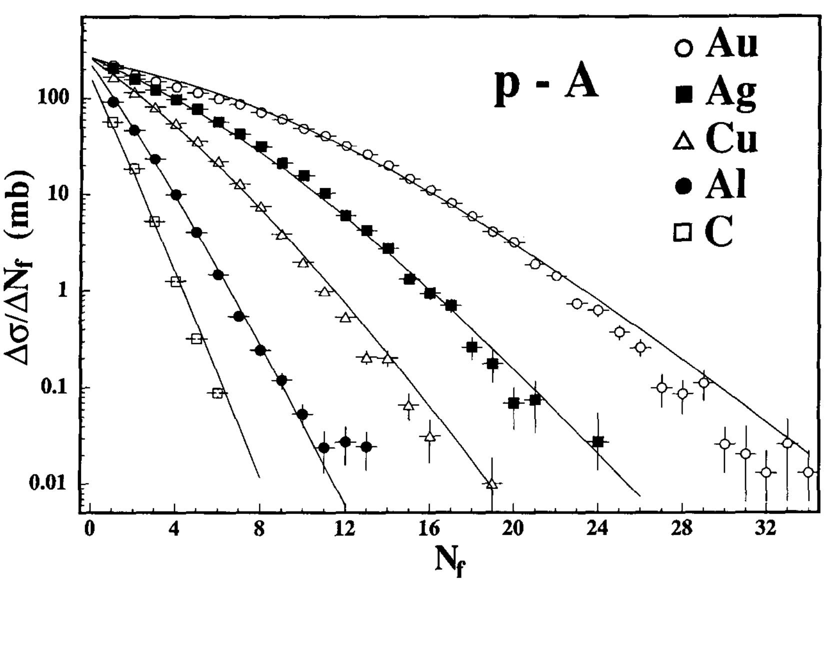

Fig. 1. Distributions of slow singly charged fragments N_f from minimum bias proton induced reactions on a variety of targets ranging from carbon to gold. The curves are fits, made with the GCM-model described in the text. The error-bars represent statistical errors

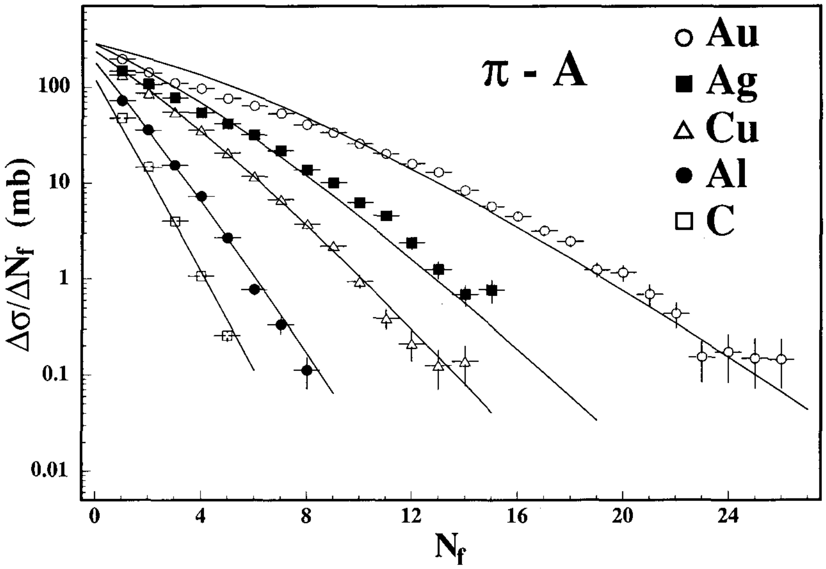

Fig. 2. Distributions of slow singly charged fragments N_f from minimum bias pion induced reactions on a variety of targets ranging from carbon to gold. The curves are fits, made with the GCM-model described in the text. The error-bars represent statistical errors

nuclei formed by nucleons placed randomly in a Woods-Saxon potential [17, 18]. To achieve the N_f – distributions for $\nu=2, 3, 4 \ldots$, the geometric distribution given in (1) was folded ν times, yielding (3) which is easily recognizable as a negative binomial. The final N_f-distribution, given by (4), is then obtained by adding all $P(N_f)$ distributions weighted according to the ν-distribution.

$$P_\nu(N_f)=\binom{N_f+\nu-1}{N_f}(1-X)^\nu X^{N_f} \tag{3}$$

$$P(N_f)=\sum_{\nu=1}^{\nu_{\max}} \pi(\nu)\cdot P_\nu(N_f). \tag{4}$$

The resulting distribution was fitted to the experimental distribution of slow protons using $\langle N_f\rangle_{\nu=1}$, as the only free parameter. The fit is done with the first two bins excluded from the fit, as these are highly dependent on background corrections and susceptible to trigger influence. Although suffering slightly from the inaccuracy in the absolute cross section determination, the model gives a fairly good description of the spectra for all the targets. The fits are shown as lines in Fig. 1 and 2.

3.1 The mass dependence of slow proton production

The target dependence of slow proton production and related quantities can be seen in Table 2 where the following mean values can be found:

Table 2. Target dependencies for slow proton related quantities. Where not indicated the systematic errors are less than 1%

Projectile		C	Al	Cu	Ag	Au	α
p	$\langle N_f\rangle$	0.66	1.06	1.94	2.93	4.55	0.72 ± 0.01
	$\langle\nu\rangle$	1.66	2.09	2.65	3.10	3.68	0.28 ± 0.01
	$\langle N_f\rangle_{\nu=1}$	0.28	0.40	0.68	0.90	1.23	0.56 ± 0.02
π	$\langle N_f\rangle$	0.65	1.00	1.69	2.48	3.67	0.63 ± 0.01
	$\langle\nu\rangle$	1.45	1.76	2.19	2.47	2.90	0.24 ± 0.01
	$\langle N_f\rangle_{\nu=1}$	0.33	0.44	0.69	0.83	1.19	0.47 ± 0.05

$\langle N_f\rangle$ = The average number of slow protons produced in an interaction.
$\langle\nu\rangle$ = The average number of leading hadron-nucleon collisions in an interaction.
$\langle N_f\rangle_{\nu=1}$ = The average number of fragments produced in each leading hadron-nucleon subcollision extracted through the GCM-model.

The target dependence has been parametrized as A^α. When the GCM-model is applied to the data the two first bins are excluded because of the large background corrections and their sensitivity to any trigger bias. The values of α for $\langle N_f\rangle_{\nu=1}$ are similar for proton and pion induced reactions, indicating that the cascading in these two cases behave very much in the same way. This is expected since the main difference between proton and pion induced reactions are the number of leading hadron-

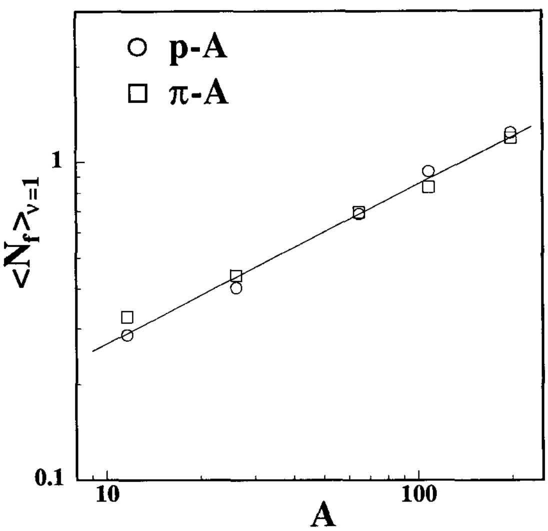

Fig. 3. The average number of slow protons produced in any projectile-target nucleon collision $\langle N_f\rangle_{\nu=1}$ extracted through the "geometric cascade model" studied as a function of the target mass A. The line represents the function const $\cdot A^{1/2}$

nucleon subcollisions, $\langle \nu \rangle$, and $\langle N_f \rangle_{\nu=1}$ is the average contribution from each subcollisions.

We found that $\langle N_f \rangle_{\nu=1}$ depends on the target-mass roughly as $\sqrt{A}$. A dependence like $A^{1/3}$ would be expected for a very limited intranuclear cascade, i.e. only the nucleons excited by the projectile are able to knock out other nucleons. The number of slow protons should then be proportional to the distance that the struck nucleon would have to travel through the remaining target. The larger value found here indicates that a nucleonic cascade is present and this is in reasonable agreement with earlier findings [19]. For the average number of slow protons per interaction, $\langle N_f \rangle$, one observes some difference between proton and pion induced reactions, Table 2. The difference here can be attributed to the difference in the elementary cross section for protons and pions.

3.2 Model comparisons

We have also compared our data to the results of the Monte Carlo model VENUS 3.11, chosen since it includes a treatment of the reinteraction of decay products from string fragmentation among themselves or with spectator nucleons [20], and the FRITIOF 1.7 model that does not contain any rescattering [18]. To compare our data to the model calculations, an experimental filter has been applied to the models, taking into account the absorption of particles in the target foil and the target chamber. Furthermore the models do not handle the production of heavier fragments, deuterons and tritons, but only protons. The models are not able to reproduce the experimental distributions for p-Au, as seen in Fig. 4, nor are they able to describe the distribution for p-C collisions. With an increase of the "baryonsize"-parameter in VENUS that model gives a descent description of the data (this parameter is the distance between two "pointlike" baryons which is the limit below which a secondary interaction will occur). A value of 3.4 fm, which is much larger than the default parameter 1.5 fm, is required to make the model fit the slow proton distribution. Such a large value seems however to be unphysical.

3.3 Angular distributions of slow protons

As mentioned above in order to limit the effect of background contributions only interactions with a transverse energy > 5 GeV are considered here. This has been taken into account also in the model calculations. Furthermore because only proton spectra are calculable in the model we limit the studies to slow protons identified in the plastic ball (i.e. the deuterons and tritons are omitted). The angular distributions are shown in Fig. 5 and it is found that the shape is relatively well described by the form $e^{\kappa \cdot \cos\theta}$, with the parameter κ being roughly 0.8 for the heavier targets but rising for the lighter ones. That the lighter targets have a more forward peaked structure is easily understood as they are not large enough for a cascade to become fully developed. For the heavier targets κ is rather constant, and only a small change is found when going from copper to heavier targets. When similar studies were performed for hadron induced reactions on emulsion at widely different energies it was found that κ had a value of 0.96, independent of energy [21]. Our definition of slow protons and what is called grey tracks in emulsion are however not selecting exactly the same

Table 3. The values for exponential fits to the angular distribution $e^{\kappa \cdot \cos\theta}$, for both the model and the experiment

Target	κ Data	κ Venus
Au	0.75 ± 0.01	1.66 ± 0.01
Ag	0.79 ± 0.01	1.67 ± 0.01
Cu	0.85 ± 0.01	1.73 ± 0.01
Al	1.00 ± 0.01	1.89 ± 0.01
C	1.32 ± 0.01	2.21 ± 0.02

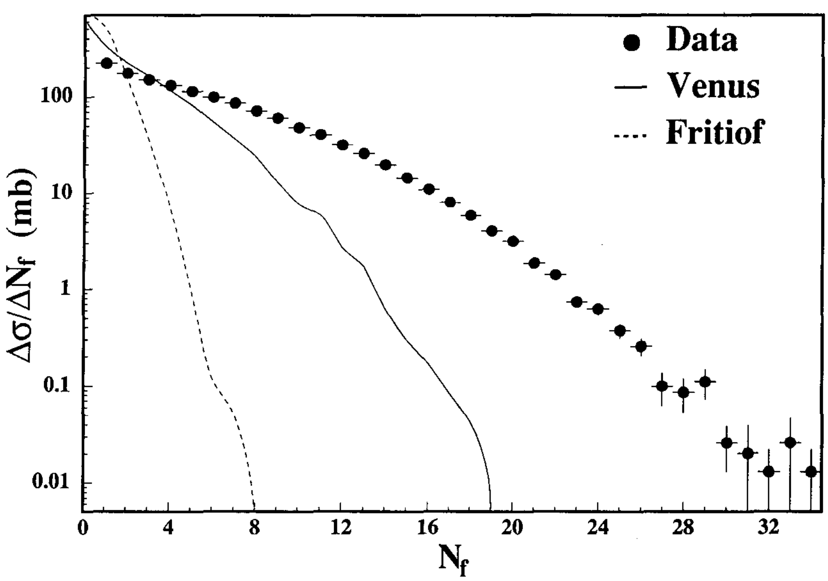

Fig. 4. The data compared to the models for proton induced reactions on gold. The solid line is the results of VENUS with it's standard parameters, and the dashed line represents the FRITIOF results

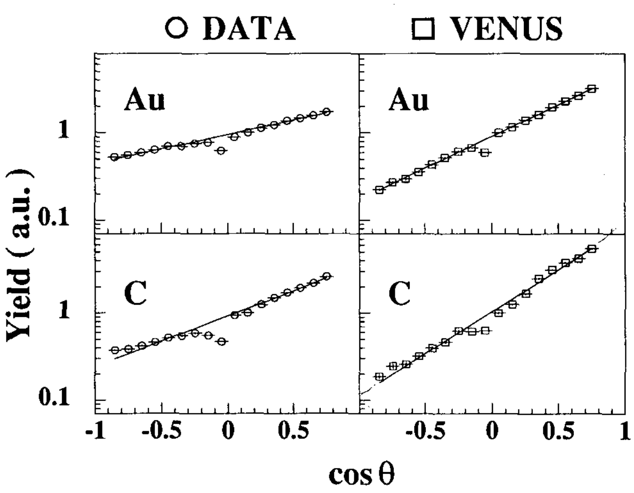

Fig. 5. The angular distributions of protons for proton induced reactions on gold and carbon. Data and the VENUS calculations are compared. The lines are fitted exponentials, see Table 3. The drop due to absorption in the experimental setup around 90° can be clearly seen

particles. Grey tracks are belived to contain in the region of 10% pions and might select protons in a different energy interval as well. The trend is the same for the VENUS model, but the slopes are approximately twice as steep as can be seen in Table 3 and Fig. 5.

3.4 Energy distributions of slow protons

As in the last paragraph only protons from interactions with transverse energy in excess of 5 GeV have been used in the following analysis. When the energy distributions of protons are investigated they are found to have the form, e^{-E/E_0}, in the interval 80–400 MeV. The reason for the energy cutoff at 80 MeV for this examination is that the energy is not unambiguously determined in the region 30–60 MeV. This does not affect the results for N_f and θ distributions studied earlier in this paper. The energy of the protons are determined from ΔE measurements in the plastic ball, giving quite large uncertainties in the energy determined for the punch-through protons ($E > 250$ MeV). This has the effect of making the experimental distribution flatter and might thus increase the extracted E_0 value. Because of this we have limited the region of our slope determination so that we use only protons of energies up to 350 MeV. We observe an angular dependent energy spectrum as seen in Table 4 and Fig. 6. This angular dependence is stronger in VENUS than in the experiment. The bump in the experimental distribution that can be seen in Fig. 6 is due to contamination of high energy deuterons in the the proton spectra, and as expected it is not as prominent in the backward hemisphere. This region were also excluded when the fits were performed. The E_0 values presented in Table 4 show no target dependence, indicating that for the lighter targets the backward protons are produced by the same mechanism as for the heavier, although the yield is smaller.

Table 4. The values for exponential fits to be energy distribution, e^{-E/E_0}, in the energy range 80–400 MeV for both the model and the experiment

Target	Angular interval	Data E_0(MeV)	Venus E_0(MeV)
Au	60°– 90°	55 ± 1	119 ± 3
	90°–120°	49 ± 2	82 ± 3
	120°–160°	44 ± 2	64 ± 4
Ag	60°– 90°	48 ± 1	118 ± 3
	90°–120°	41 ± 2	82 ± 3
	120°–160°	40 ± 3	65 ± 3
Cu	60°– 90°	57 ± 1	115 ± 3
	90°–120°	52 ± 3	84 ± 3
	120°–160°	46 ± 3	64 ± 4
Al	60°– 90°	60 ± 1	117 ± 3
	90°–120°	53 ± 4	80 ± 3
	120°–160°	48 ± 7	52 ± 4
C	60°– 90°	49 ± 1	111 ± 3
	90°–120°	42 ± 1	73 ± 5
	120°–160°	41 ± 4	55 ± 20

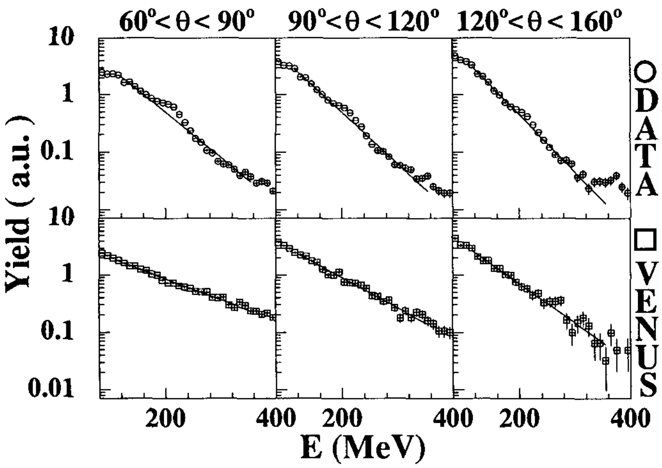

Fig. 6. Energy distributions for proton induced reactions on gold for three different θ-bins. Data and the VENUS model are compared. The lines are exponential fits, see Table 4

The distributions produced by VENUS have similar shapes, but the E_0-values are considerably larger and thus the energy distributions extend to higher energies. The experiment exhibit a much stronger intranuclear cascade than VENUS, an interpretation that is in agreement with the result for angular distributions studied in Sect. 3.3.

4 Conclusions

The distributions of slow singly charged fragments in proton and pion induced interactions at 200 GeV/c can be reasonably well understood in terms of a "geometric cascade model". The data indicates that we have a relatively large intranuclear cascade, as the average multiplicity of produced fragments, normalized to the number of target participants clearly shows a dependence that is stronger than $A^{1/3}$. Neither FRITIOF nor VENUS produce enough slow protons in comparison with the experimental observations. The energy distributions of slow protons exhibit angular but not target mass dependence. The angular distributions however exhibit a clear target mass dependence but the difference is fairly small for nuclei of mass greater than 70. This seems to indicate that already a copper nucleus is big enough for the cascade in the nuclear medium to fully develop.

Acknowledgements. We thank the accelerator division of CERN for their excellent work. The partial support by the German BMFT and DFG, the United States DOE, the Swedish NFR and the Humbolt Foundation is gratefully acknowledged.

References

1. W.D. Shephard et al.: Proc of the XVIII Int. Symp. on Mult. Part. Dyn. 1987 and references therein, I. Dremin, K. Gulamov (eds.), p. 231. Singapore: World Scientific 1988
2. S.P. Sorensen et al.: Z. Phys. C – Particles and Fields 38 (1988) 3
3. B. Andersson, I. Otterlund, E. Stenlund: Phys. Lett. 73B (1978) 343; E. Stenlund, I. Otterlund: Nucl. Phys. 198B (1982) 407
4. M.K. Hegab, J. Hüfner: Phys. Lett. 105B (1981) 103
5. W. Busza: Proc. of the XV Int. Symp. on Mult. Part. Dyn. 1984, p. 66, G. Gustafson, C. Petersson (eds.). Singapore: World Scientific 1984
6. J.L. Bailly et al.: Z. Phys. C – Particles and Fields 35 (1987) 301
7. E.G. Boos et al.: Z. Phys. C – Particles and Fields 26 (1984) 43
8. C. De Marzo et al.: Phys. Rev. D29 (1984) 2476
9. C.D. Rees et al.: Z. Phys. C – Particles and Fields 17 (1983) 95
10. M.A. Faessler et al.: Nucl. Phys. 157B (1979) 1; K. Braune et al.: Z. Phys. C – Particles and Fields 13 (1982) 191
11. R. Albrecht et al. (WA80 Coll.): Z. Phys. C – 45 (1990) 529
12. R. Albrecht et al. (WA80 Coll.): Report No. GSI-85-32
13. R. Albrecht et al.: Nucl. Instrum. Methods 276 (1989) 131
14. T.C. Awes et al.: Nucl. Instrum. Methods A279 (1989) 479
15. A. Baden et al.: Nucl. Instrum. Methods 203 (1982) 189
16. E.B. Brucker et al.: Phys. Rev. D32 (1985) 1605
17. G. Nilsson, E. Stenlund: LUIP 8001
18. B. Nilsson-Almquist, E. Stenlund: Comp. Phys. Commun. 43 (1987) 387
19. P. Zavada: Phys. Rev. C40 (1989) 285
20. K. Werner, P. Koch: Phys. Lett. 242B (1990) 251
21. I. Otterlund et al.: Nucl. Phys. 142B (1978) 445